Formation and Corrosion Behavior of Nickel/Alumina Nanocomposites

D.I. Tishkevich[1,2,a*], A.I. Vorobjova[3,b] and D.A. Vinnik[2,c]

[1]SSPA "Scientific and Practical Materials Research Centre of NAS of Belarus", Minsk, Belarus
[2]South Ural State University, Chelyabinsk, Russia
[3]Belarussian State University of Informatics and Radioelectronics, Minsk, Belarus

[a]dashachushkova@gmail.com, [b]vorobjova@bsuir.by, [c]denisvinnik@gmail.com

Abstract. Ni nanopillars (Ni NPs) composite materials formation technology was presented. The morphological and structural properties of the composite material were investigated using scanning electron microscopy, atomic force microscopy, X-ray diffraction. The corrosion resistance of the nanocomposite materials has been studied by potentiodynamic polarization curves analysis. The composite represents the array of vertically ordered Ni NPs with the identical size in alumina matrix. XRD investigation indicates that Ni NPs are polynanocrystalline material. It has been shown that Ni NPs and the composite material have sufficient corrosion resistance in a 0.9% aqueous NaCl solution. Porous alumina matrix is the neutral and protective component of the composite. These nanocomposite materials can be excellent candidates for practical use in different applications.

Introduction

Porous anodic alumina matrices are widely used as templates for the magnetic composite materials formation due to their unique properties [1,2]. Many studies of magnetic materials obtained by electrochemical deposition in porous anodic alumina are due to their potential applications in computer read/write heads, microelectromechanical systems, biosensor devices and integrated circuits. In all application, the magnetic layers must have good adhesion, high corrosion resistance and thermal stability. New nanostructured composite materials based on nanoscale structural elements: nanopillars, nanotubes, nanowires or nanodots are developed and researched to ensure such properties [3,4]. The nanostructured materials are finding more different applications because of their unusual mechanical, optical, magnetic, chemical and catalytic properties [9-15]. The electrodeposited Ni films were widely used to improve mechanical and corrosion properties of Al, Mg, Cu and other alloys. And most of the articles relate to corrosion behavior of conventional bulk Ni-based alloys and coatings [5,6]. The papers about corrosion behavior of nanostructured Ni-composites or coatings is limited [7]. Only a few recent studies have shown that nanocrystalline Ni thin films can also successfully use as a corrosion protective coating [8,9]. The passive state of bulk Ni in an alkaline and acid environment was considered in detail in works [9,10]. Ni electrochemical behavior, including in the composition of thin-film composite and template-assistant materials in salts aqueous solutions has not been practically studied.

The objectives of this work are the formation process study of Ni-based composite material nanopillars in the anodic alumina matrix and corrosion resistance study of obtained composite material in sodium chloride aqueous solutions.

Experimental

Experimental samples were two-layer thin-film compositions of Al and Ti, deposited on Si/SiO$_2$ (d=76 mm) substrates. Al films with 1000 ± 50 nm thickness and Ti with 400 ± 50 nm thickness were deposited by electron beam sputtering in the Oratoriya-9 equipment. Porous anodic alumina (PAA) thin films with an ordered structure were obtained by two-stage anodizing method in 4% H$_2$C$_2$O$_4$ in a potentiostatic regime at a 40V and 14°C electrolyte temperature. Anodizing process was carried out in a two-electrode cell. A graphite plate was used as an auxiliary electrode, and the electrolyte was mixed with a magnetic stirrer. The removal process of the barrier layer at the PAA pores bottom was

performed as described in [1,3,11]. This matrix has the following parameters: PAA height – 1.3 ± 0.05 μm, pore diameter from 65 ± 5 nm to 75 ± 5 nm, matrix step 105 ± 5 nm.

The Ni electrodeposition was carried out in a two-electrode cell by potential sweeping at 20 mV/s constant rate from zero to a constant potential in the range from -1.6 V to -2.2 V and then, at this potential for 3.0 to 10 min (DC-deposition). Anodizing, etching and electrochemical deposition processes were controlled using the Electronic Measurements Galvanostatic/Potentiostatic power supply P-5827 M. An electrolyte of the following composition was used (g/l): $NiSO_4 \times 7H_2O$ (140) + $NiCl_2 \times 6H_2O$ (30) + H_3BO_3 (25) + Na_2SO_4 (60).

The morphology of experimental samples were investigated using scanning electron microscopy (SEM – Philips XL30SFEG) and AFM (Nanotop NT-206). Samples were processed in a selective etching solution for alumina before SEM and AFM studies. Alumina was removed by selective chemical dissolution in the mixture: 35 ml/l 85% H_3PO_4 + 20 g/l CrO_3 at 80 ± 2 °C for 3 minutes.

Samples phase composition was investigated by X-ray diffraction (XRD) method using a DRON-2 diffractometer with Cu Kα radiation (λ=0.154 nm).

Electrochemical studies of the composite material were performed by AUTOLAB PGSTAT302n Potentiostat/Galvanostat. Data processing was carried out using NOVA software (version 1.10). The linear polarization method was used for currents and corrosion potentials measuring in a potentiodynamic regime at a 1.0 mV/s potential scan rate. Samples were kept in solution without polarization for 2-3 min before the polarization curves registration. The initial value of the polarization potential at potentiodynamic polarization curves (PPC) was automatically set to 100 mV more negative than the open circuit potential. PPC were recorded in the +500 to -450 mV range and 1–100 mV/s sweep rates. Corrosion resistance properties studies were performed in a 0.9% NaCl aqueous solution. The electrolyte acidity was 6.14±0.02 pH.

Thus, two systems of samples were obtained for the electrochemical measurements: Ti/Al_2O_3 and $Ti/Al_2O_3/Ni$.

Results and Discussion

Figure 1 shows the samples SEM surface images after Ni electrochemical deposition in PAA at a constant potential within 8 min (a) and 5 min (b) after alumina etching at a -1.8 V. Insert in Fig. 1 shows a cross-section formation scheme, explaining how cross-section is formed and why alumina selective etching is necessary [31]. Cross-section is usually formed not in the center (middle of the pillars chain, black arrow), but along the oxide cells edge (red arrow). Additionally, the mechanical damage of the surface fracture occurs during cross-section obtaining due to the oxide consists domains with an ordered structure.
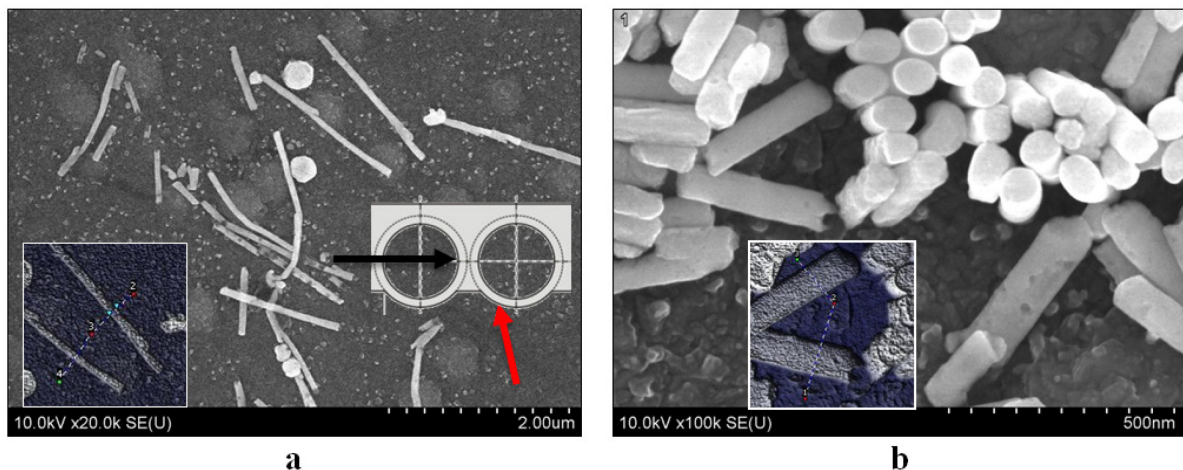

Fig. 1. Samples SEM images obtained in the Ni deposition DC regime and after alumina selective etching: a – at -1.8 V constant potential within 8 min; b – at -1.8 V constant potential within 5 min.

However, there are boundaries between domains along which a cross-section appears. Therefore, we cannot see the pillars on the cross-section, despite the fact that the surface SEM image shows that they are. The distance between the pores (pillars), or cell diameter, for all samples was estimated by the formula $D_c = k \cdot U_a$, $= 2.6$ nm/V $\cdot$ 40 V $= 104$ nm and by surface SEM images [31]. The presented method for composite material formation, including two-stage anodizing and subsequent modification of PAA with a combination of electrochemical thinning and selective chemical etching, allows to obtain a thin-film matrix with an ordered structure and a planar metal-oxide interface not separated from the substrate.

The presented method allows to obtain a thin-film matrix with an ordered structure and a planar metal-oxide interface not separated from the substrate. Near the barrier layer (border with Ti) the pores are almost 100% filled. Figure 2 shows AFM samples surface images after Ni deposition for a short duration (3 min) and oxide removal. During this time, Ni fills almost all the pores on the inner border with Ti.
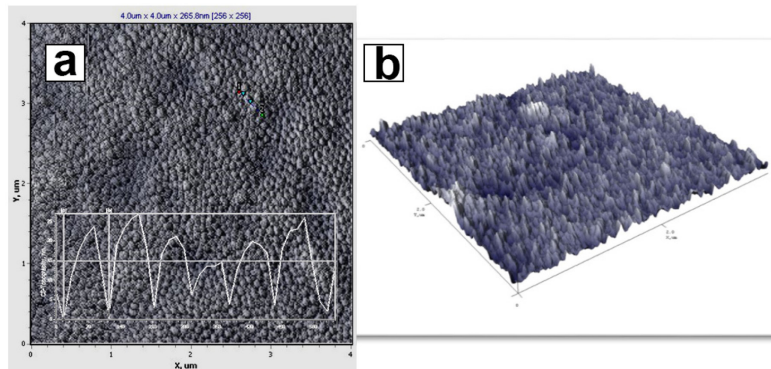

Fig. 2. 2D (a) and 3D (b) AFM images and sample surface after Ni deposition in following regime: deposition potential -1.6 V, deposition time 3 min.

The Ni phase is crystallized in face-centered cubic (fcc) lattice, as evidenced by identification of Ni samples with diffraction lines of reference powder Ni (according to powder diffraction file JCPDS 01-1260). Except the main peak of a magnetic phase at 43.67° (111), there are two weaker peaks at 50.9° and 74.9° which correspond to crystal orientation (200) and (220). As it is reported in [12], these orientations are specific for electrodeposited into alumina template Ni NPs. The primary direction of Ni growth in alumina pores is the orientation (111), and height of the corresponding peak is significantly larger than for other peaks. It shows a high crystallinity of NPs and mutual crystallites orientation along the main growth direction. Other weak peaks existence shows the presence of small crystallites amount with other growth directions.

The typical XRD pattern of DC-electrodeposited Ni NPs in the PAA is presented in Figure 3.
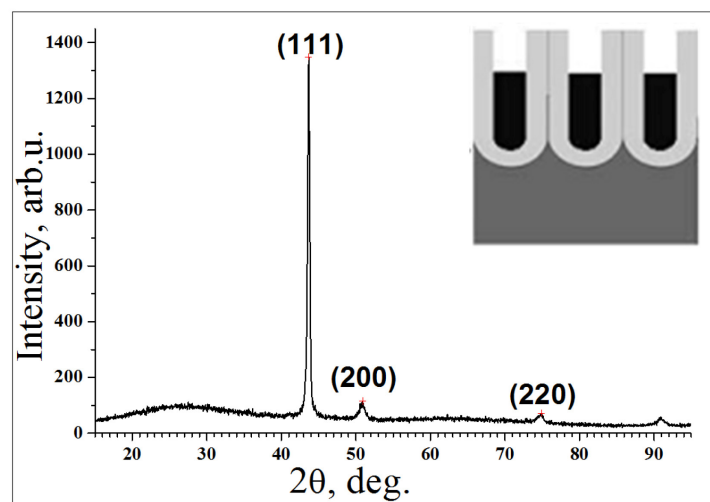

Fig. 3. XRD-spectra of Ni-PAA nanocomposite material.

Figure 4 shows the PPC of the Ti/Al$_2$O$_3$/Ni electrode (1) and Ti/Al$_2$O$_3$ electrode before barrier layer selective etching (2). In fact, the second sample is the Al$_2$O$_3$ – electrolyte interface, that is, it characterizes the electrochemical behavior of anodic alumina. From the PPC 1 were determined the template passivation parameters, i.e., start passivation potential (E$_{sp}$ = -0.5V), complete passivation potential (E$_{cp}$ = -0.37V), and passivation current density (J$_{pass}$ = 0.78·10^{-3}µA/cm^2). From the PPC 1 were determined the template passivation parameters, i.e., start passivation potential (E$_{sp}$ = -0.5V), complete passivation potential (E$_{cp}$ = -0.37V), and passivation current density (J$_{pass}$ = 0.78·10^{-3} µA/cm^2). It can be seen from these data that alumina in this potential range is passive and makes an insignificant contribution to the sample corrosive current.
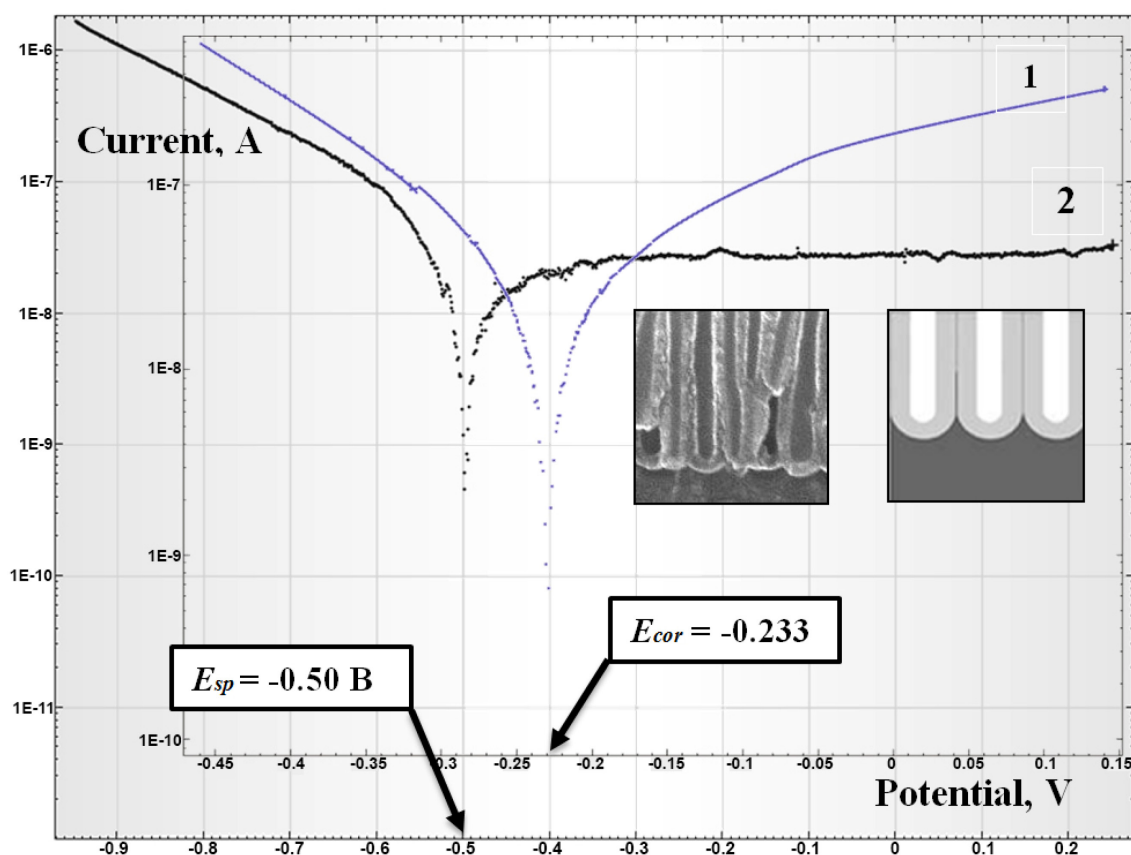

Fig. 4. PPCs of Ti/Al$_2$O$_3$/Ni electrode (1) and Ti/Al$_2$O$_3$ electrode (2).

In addition, in these experimental conditions, when could be realized the corrosion electrochemical mechanism during the galvanopair (Ti/Ni) creation, the actual corrosion does not occur. The commonly used method for the corrosion rate and resistance analyzing of various alloys and composites is the PPC analysis. The simplest express-method for the corrosion current density determining is to extrapolate the polarization curve straight-line portion (cathodic and anodic) in semi-logarithmic coordinates (Tafel PPC) to the corrosion potential E$_{corr}$. In this case, the intersection points of the anodic and cathodic PPC in Tafel coordinates (lgI – E) determine the corrosion current potential and density.

Figure 5 demonstrates the PPCs of Ti/Al$_2$O$_3$/Ni electrodes in a 0.9% NaCl aqueous solution at 0.1 V/s potential sweep rate in semi-logarithmic coordinates. However, as Ni is inclined to passivation, for receiving linear Tafel regions on PPC, experiments were performed immediately after immersion of the prepared samples in the electrolyte. It is necessary to avoid passivation and to understand the corrosion resistance of fresh nanocrystalline Ni NPs surface in alumina. Table 1 shows the parameters characterizing the corrosion process of identical experimental samples, obtained by extrapolating the polarization curves. For comparison, the table also presents data for metallurgical Ni, a continuous thick Ni film obtained by electrochemical deposition, and a thin nanocrystalline Ni film obtained by magnetron sputtering [13-16].
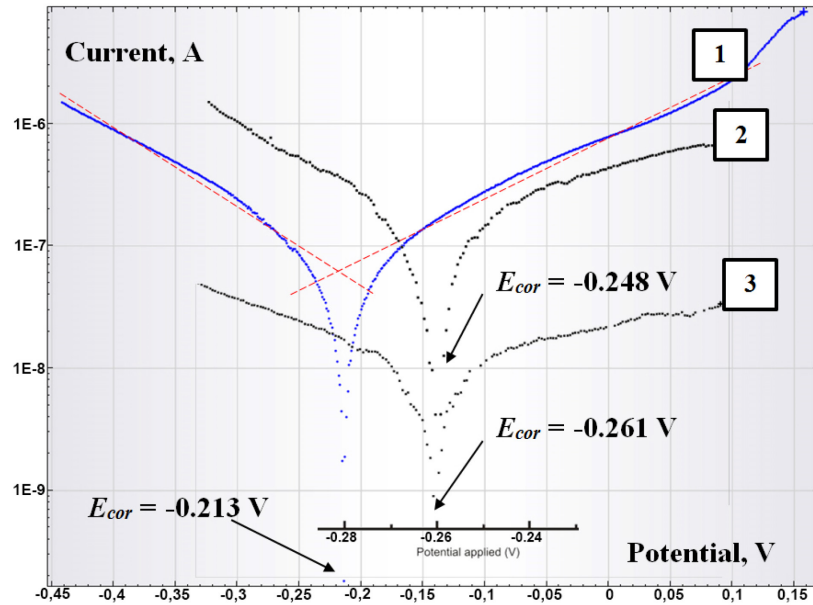
Fig. 5. PPCs of Ti/Al$_2$O$_3$/Ni electrode in semi-logarithmic coordinates: 1 – immediately after immersion; 2, 3 – PPCs of identical samples after the third and fifth cycles of polarization.

Table 1. The corrosion parameters of Ti/Al$_2$O$_3$/Ni composite, determined by the polarization curves extrapolation method.

Sample	E_{corr}, V	I_{corr}, µA	J_{corr}, µA /cm^2	b_a, mV/decade	b_c, mV/decade
Ti/Al$_2$O$_3$/Ni (1)	-0.213	$1.23 \cdot 10^{-3}$	$6.53 \cdot 10^{-2}$	–	–
Ti/Al$_2$O$_3$/Ni (2)	-0.213	$1.68 \cdot 10^{-3}$	$8.06 \ 10^{-2}$	68	90
Ni [13] nano	-0.239	–	$3.9 \cdot 10^{-2}$	–	–
Ni [14] bulk	-0.263	–	$37.5 \cdot 10^{-2}$	–	–
Ni [14] bulk electrodeposited	-0.303	–	$222.6 \cdot 10^{-2}$	185	273
Ni [15] bulk nano	-0.494	–	$521 \cdot 10^{-2}$	–	–
Ni [16] bulk	-0.428	–	$705.9 \cdot 10^{-2}$	–	–

It can be seen from the Table 1 that Ni nanopillars protected by alumina are more resistant to dissolution processes than massive, metallurgical nickel [16] or electrochemically deposited thick nickel films [14]. This is evidenced by the fact that the films corrosion potential is shifted to a positive region, and the corrosion currents are several orders of magnitude lower. It is known that nanomaterials prepared by mechanical method contain a lot of pores and microstrains in the grain boundary region, which are more prone to corrosion attack. However, nanomaterials prepared by electrodeposition method are mostly compact and does not contain a pores [15]. Thin-film nanocrystal materials (Ni nanocrystalline thin films [15]) and studied composite Ti/Al$_2$O$_3$/Ni are showed comparable results taking into account the crystallites sizes and somewhat different conditions of experiment.

Conclusions

The formation method of a composite material based on Ni nanopillars embedded in porous alumina matrix using electrochemical processes is examined. The results of the morphological, structural and corrosion properties of the obtained composite material are given. It is shown that the

formation method of porous alumina matrix affects at the nanopillars morphological parameters. Two-stage anodizing and the subsequent PAA modification with an electrochemical thinning and selective chemical etching combination make it possible to obtain a thin-film matrix with an ordered structure and a planar metal-oxide interface. This contributes to improve the metal electrochemical deposition conditions at the same time in most pores and improves the deposition uniformity, not only in height, but also in the sample area.

The results of the experimental PPC analysis are presented using extrapolation of the PPC straight-line portion in semi-logarithmic coordinates (cathode and anodic) to the corrosion potential E_{corr} and Tafel coefficients determining. PAA is not only a shape template, but also performs protective functions. PPC method showed that the $Ti/Al_2O_3/Ni$ composite material corrosion resistance is due to matrix protective properties, which in this potential range is the neutral and protective component of the composite. The electrochemical corrosion mechanism of galvanopair Ti/Ni is also not realized since there are no pores or cracks in the compact composite material and Ti or Al ions mass transfer into the liquid phase is almost impossible. Generally, it has been experimentally shown that the obtained nanocomposite materials have a good corrosion resistance in -450 to +450 mV potentials range in the studied electrolyte, which is widely used in biomedical and other new materials corrosion studies. The electrochemical properties study of this nanocomposite material will improve the technology of its production and predict the long-term stability of structures based on it (biosensors sensitive elements, magnetic memory elements, nanoemitters in liquid crystal display devices, etc.).

Acknowledgments

References

[1]   A.I. Vorobyova, E.A. Outkina, O.M. Komar, Study of metal pillar nanostructure formation with thin porous alumina template, Thin Sol. Films, 548 (2013) 109-117.

[2]   Y. Zhang, M. Zhang, Z. Cai, M. Chen, F. Cheng, A novel electrochemical sensor for formaldehyde based on palladium nanowire arrays electrode in alkaline media, Electrochim. Acta, 68 (2012) 172-177.

[3]   A.I. Vorobyova, E.A. Outkina, A.A. Khodin, Nickel/Alumina nanocomposites by ac electrochemical processing, Appl. Phys. A. Mater. Sci.& Proces. 122 (2016) 1-11.

[4]   M.P. Proenca, C.T. Sousa, J. Ventura, M. Vazquez, J.P. Araujo, Distinguishing nanowire and nanotube formation by the deposition current transients, Nanoscale Res. Lett. 7 (2012) 1-9.

[5]   G.Z. Meng, L. Yang, Y.W. Shao, Effect of microstructures on corrosion behavior of nickel coatings: (II) competitive effect of grain size and twins density on corrosion behavior. J. Mater. Sci. Technol. 32 (2016) 465–469.

[6]   D.I. Tishkevich, S.S. Grabchikov, L.S. Tsybulskaya, V.S. Shendyukov, S.S. Perevoznikov, S.V. Trukhanov, E.L. Trukhanova, A.V. Trukhanov, D.A. Vinnik, Electrochemical deposition regimes and critical influence of organic additives on the structure of Bi films, J. of All. and Comp. 735 (2018) 1943-1948.

[7]   L.P. Wang, J.Y. Zhang, Y. Gao, Q.J. Xue, L.T. Hu, T. Xu, Grain size effect in corrosion behavior of electrodeposited nanocrystalline Ni coatings in alkaline solution, Sc. Mater. 55 (2006) 657-660.

[8]   S. Goodwin, C. Peterson, C. Hoh, C. Bittner, Targeting and retention of magnetic targeted carriers (MTCs) enhancing intra-arterial chemotherapy, J. Magn. Magn. Mater. 194 (1999) 132-139.

[9].   J. Liu, X. Zhu, J. Sudagar, W. Diao and S. Yu, Increased corrosion resistance of closed-cell aluminum foams by electroless Ni-P coatings, Mater. Trans. 52 (2011) 2282-2284.

[10]   Y. Hirota, Y. Akiyama, Y. Izumi, and S. Nishijima, Fundamental study for development magnetic drug delivery system, Phys. C Supercond. its Appl. 469(2009) 1853–1856.

[11]   D.L. Shimanovich, A.I. Vorobjova, D.I. Tishkevich, A.V. Trukhanov, M.V. Zdorovets, A.L. Kozlovskiy, Preparation and morphology-dependent wettability of porous alumina membranes, Beilstein J. Nanotechnol. 9 (2018) 1423-1436.

[12]   H. Pan, B. Liu, J. Yi, C. Poh, S. Lim, J. Ding, Y. Feng, C.H.A. Huan, J. Lin, Growth of single-crystalline Ni and Co nanowires via electrochemical deposition and their magnetic properties, J. Phys. Chem. B. 109 (2005) 3094.

[13]   M. Danişman The corrosion behavior of nanocrystalline nickel based thin films, Mater. Chem. Phys. 171 (2016) 276-280.

[14]   B.I. Onyeachu, X. Peng, E.E. Oguzie, C.E. Ogukwe, I. Digbo, Characterizing the electrochemical corrosion behaviour of a Ni–28wt.%Al composite coating in 3.5%NaCl solution, Port. Electrochim. Acta. 33 (2015) 69-83.

[15]   L.Y. Qin, J.Sh. Lian, Q. Jiang, Effect of grain size on corrosion behavior of electrodeposited bulk nanocrystalline Ni, Trans. Nonferrous. Met. Soc. China. 20 (2010) 82–89. doi:10.1016/S1003-6326(09)60101-1.

[16]   X. Wang, B. Wang, L. Zhang, C. Yang, Y. Yang, Effect of different welding processes on electrochemical and corrosion behavior of pure nickel in 1 M NaCl solution, Metals (Basel) 7 (2017) 532.